



Contents lists available at ScienceDirect

Taiwan Journal of Ophthalmology

journal homepage: www.e-tjo.com

Review article

Impact of swept source optical coherence tomography on ophthalmology



Shoji Kishi*

Department of Ophthalmology, Gunma University Graduate School of Medicine, Maebashi, Japan

ARTICLE INFO

Article history:

Received 15 September 2015

Accepted 29 September 2015

Available online 2 December 2015

Keywords:

Harada disease

macular hole

posterior precortical vitreous pocket

swept source optical coherence tomography

vitreoretinal interface disease

ABSTRACT

Swept source optical coherence tomography (SS-OCT) was introduced in clinical practice in 2012. Because of its deeper penetration and faster acquisition time, SS-OCT has the ability to visualize choroid, vitreous, and retinal structures behind dense preretinal hemorrhages. Swept source optical coherence tomography has positively influenced and hugely contributed to the research of the vitreous body. It is the first ophthalmic diagnostic technology to demonstrate the entire structure of the posterior precortical vitreous pocket (PPVP) *in vivo*. The roles of the PPVP in physiological posterior vitreous detachment and vitreoretinal interface disorders have now been elucidated. The presence of a connecting channel between the PPVP and Cloquet's canal suggests that the aqueous humor drains into the premacular space. Deeper penetration of SS-OCT has made it possible to view the choroid. It also has an important role in central serous chorioretinopathy and uveitis. We have also been able to treat Harada disease by monitoring the choroidal thickness by SS-OCT.

Copyright © 2015, The Ophthalmologic Society of Taiwan. Published by Elsevier Taiwan LLC. This is an open access article under the CC BY-NC-ND license (<http://creativecommons.org/licenses/by-nc-nd/4.0/>).

1. Introduction

Swept source optical coherence tomography (SS-OCT) became available in clinical practice in 2012. SS-OCT and spectral-domain optical coherence tomography (SD-OCT) are categorized as Fourier domain optical coherence tomography. The light source in SD-OCT is a super-luminescent diode, whereas the light source in SS-OCT is a tunable laser. In SD-OCT, broad wavelength light is divided into a spectrum by diffraction and thereafter it is projected to a spectroscopy where light interference is achieved. In SS-OCT, the light source is already divided into a spectrum through a tunable laser, thus a spectroscopy is unnecessary in SS-OCT (Figure 1). This simplified mechanism contributes to high-speed data acquisition that is twice as fast as that achieved by SD-OCT and it results in a clearer image. The depth of tissue penetration is governed by the wavelength of the light source used. The median wavelength of the light source in SD-OCT is approximately 840 nm. In SS-OCT, the median wavelength is 1050 nm. Swept source optical coherence tomography has enabled the visualization of the whole thickness of the choroid and structures beneath a retinal

hemorrhage or the retinal pigment epithelium (RPE). The unexpected and surprisingly detailed visualization of posterior vitreous structures has greatly improved our understanding of various vitreoretinal interface disorders. In this article, I review my recent works that used SS-OCT.

2. Differences between the images acquired by SD-OCT and by SS-OCT

A 46-year-old man presented with hazy vision in his right eye for the last 9 days. He also had tinnitus of 5 days duration. At the initial visit, his right eye showed limbal injection. Slit lamp biomicroscopy revealed cells (1+) in anterior chamber and few keratic precipitates in the same eye. The SD-OCT scanner (Cirrus HD-OCT; Carl Zeiss Meditec, Tokyo, Japan) failed to show any abnormality of the posterior fundus (Figure 2A). However, the SS-OCT scanner (DRI OCT-1 Atlantis; Topcon, Tokyo, Japan) revealed a premacular vitreous pocket, cells infiltrating in the vitreous gel, and swelling of the choroid in his right eye (Figure 2B). His left eye also showed choroidal swelling. We diagnosed the uveitis as Harada disease. Hence, SS-OCT shows superior image acquisition, which enables visualization of the vitreous and choroid.

Conflicts of interest: The author has no conflicts of interest to declare.

* Department of Ophthalmology, Gunma University Graduate School of Medicine, 3-39-15 Showamachi Maebashi, Gunma 371-8511, Japan.

E-mail address: shojikishi@gunma-u.ac.jp.

<http://dx.doi.org/10.1016/j.tjo.2015.09.002>

2211-5056/Copyright © 2015, The Ophthalmologic Society of Taiwan. Published by Elsevier Taiwan LLC. This is an open access article under the CC BY-NC-ND license (<http://creativecommons.org/licenses/by-nc-nd/4.0/>).

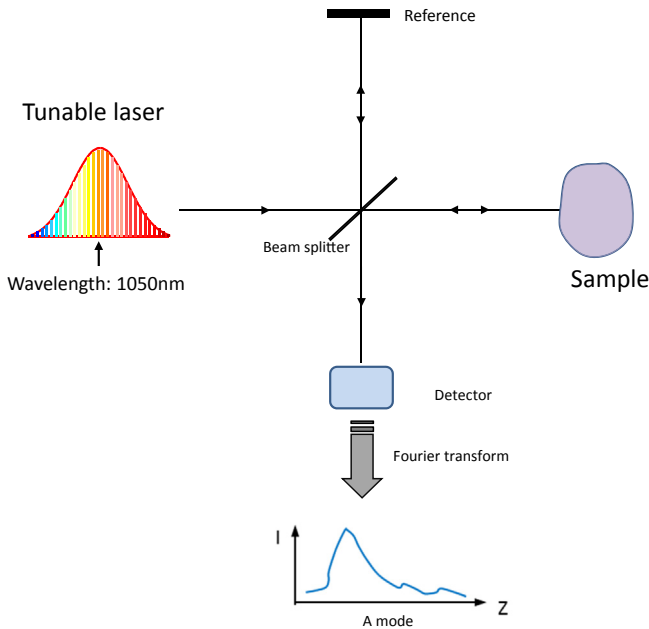


Figure 1. Schematic drawing of the swept source optical coherence tomography device. The light source is a tunable laser.

3. Posterior precortical vitreous pocket

The posterior precortical vitreous pocket (PPVP) is a premacular liquefied lacuna that is physiologically present in human eyes, except in newborns.¹ We found this structure in postmortem eyes by using fluorescein to stain the vitreous (Figure 3). Worst² was the

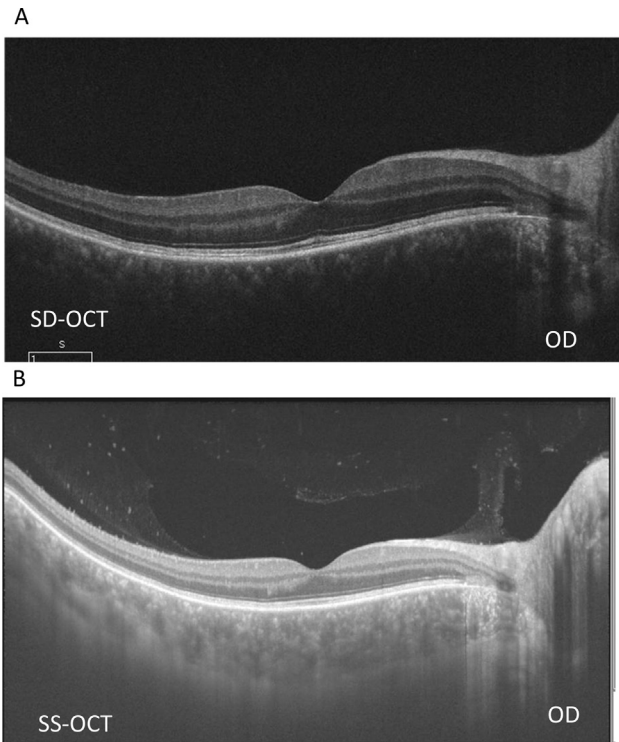


Figure 2. A comparison of the B scan images between spectral-domain optical coherence tomography (SD-OCT) and swept source optical coherence tomography (SS-OCT) in a patient with uveitis. OD = oculus dexter; SD-OCT = spectral-domain optical coherence tomography; SS-OCT = swept source optical coherence tomography.

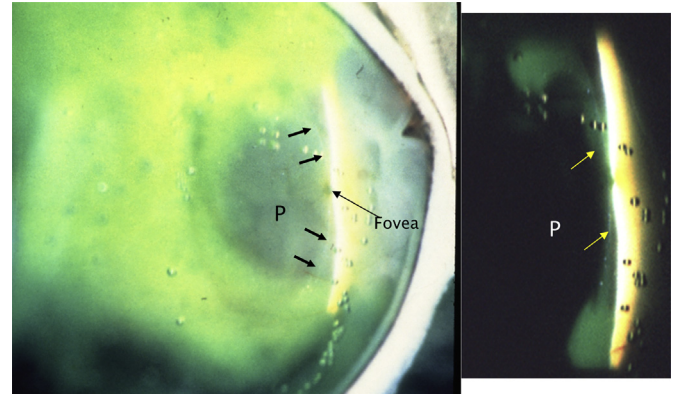


Figure 3. Posterior precortical vitreous pocket (PPVP) in a postmortem eye in which the vitreous is stained with fluorescein. The posterior wall of the PPVP is a thin layer of the vitreous cortex (arrows). P = posterior precortical vitreous pocket.

first investigator to report a premacular space in the vitreous. He injected India ink into the central vitreous and found cisterns in the vitreous of a young adult.² He described this premacular space as the “bursa premacularis.”³ According to him, the bursa premacularis was located in the convexly detached posterior vitreous cortex. He referred to the lenticular space between the focally detached vitreous cortex and the retina as the subbursal space. Based on his anatomical and morphological explanation of bursa premacularis, the vitreous cortex should always be detached from the macula. Based on his observations, we cannot explain the role of the vitreous cortex in vitreoretinal interface disorders. However, in our observation, the posterior wall of the precortical vitreous space is a thin vitreous cortex itself and the anterior border is delineated by the vitreous gel. We defined the space as the “posterior precortical vitreous pocket.”¹ Because of the PPVP, the premacular vitreous cortex is a thin collagen sheet that is separated from the gel and is spared from anterior traction by the gel. We previously described the role of the PPVP in idiopathic epiretinal membrane,⁴ proliferative diabetic retinopathy,⁵ and macular holes.⁶ Because of the gel’s transparency, the PPVP is virtually undetected during slit lamp biomicroscopy. The presence of the PPVP was further confirmed after the introduction of triamcinolone-assisted vitrectomy.^{7,8}

4. Posterior precortical vitreous pocket observed by SS-OCT

Swept source optical coherence tomography has the ability to make the PPVP visible *in vivo*.⁹ It is a boat-shaped space anterior to the posterior pole in the horizontal B scan with the patient sitting upright (Figure 4). The average height at the fovea is 0.7 mm and the width is 6.4 mm. In the vertical section, the superior portion of PPVP is elevated and the top is extended superiorly beyond the anterior limit of the B scan image. If the patient is supine, the anterior limit of the PPVP expands.¹⁰ This suggests that the humor inside the PPVP is lighter than the gel and that it is deformed by the gravity of the gel. It is surprising that a connecting channel exists between the PPVP and Cloquet’s canal (Figure 4).¹ Because Cloquet’s canal opens in the retrolental space of the posterior chamber, the aqueous humor may drain into the PPVP.

5. Evolution of the posterior precortical vitreous pocket in children

We observed the posterior vitreous in 73 normal right eyes of children (aged 3–11 y) by using SS-OCT.¹¹ The PPVP emerges in front

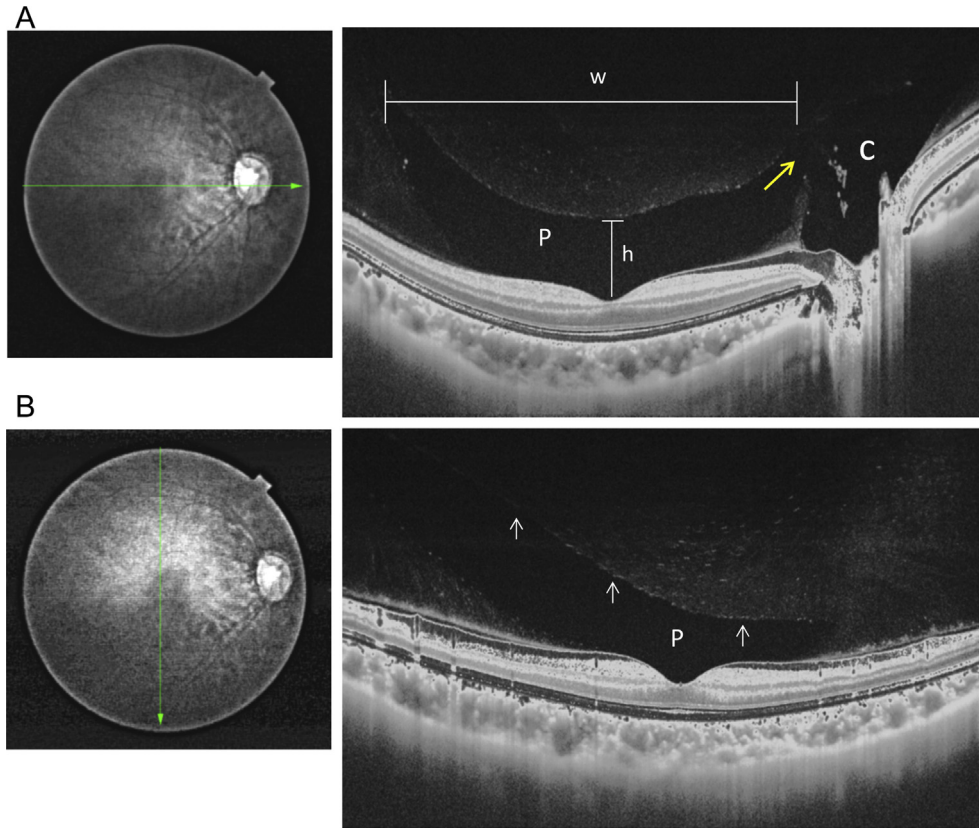


Figure 4. The swept source optical coherence tomography image of the posterior precortical vitreous pocket (PPVP) in the normal right eye of a 24-year-old female. (A) The horizontal section. The mean height (h) is 0.7 mm and the mean width (w) is 6.4 mm. There is connecting channel (yellow arrow) between the PPVP (P) and Cloquet's canal (C). (B) The vertical section. The anterior wall of the PPVP (arrows) approaches the superior portion of the PPVP. C = Cloquet's canal; h = height; P = posterior precortical vitreous pocket; w = width.

of the macula as a solitary space in early childhood. By the age of 3 years, it is in the form of a narrow liquefied space anterior to the macula, which enlarges to a small boat-shaped space with advancing age (Figure 5). The mean size of the PPVP changes from 165 μm in depth and 3327 μm in width at the age of 3 years to

524 μm in depth and 5485 μm in width after the age of 7 years. The channels connecting the PPVP and Cloquet's canal begin to appear after the age of 5 years. These findings suggest that the PPVP and the connecting channel are formed during embryologic development and their dimensions change during childhood as a child ages.

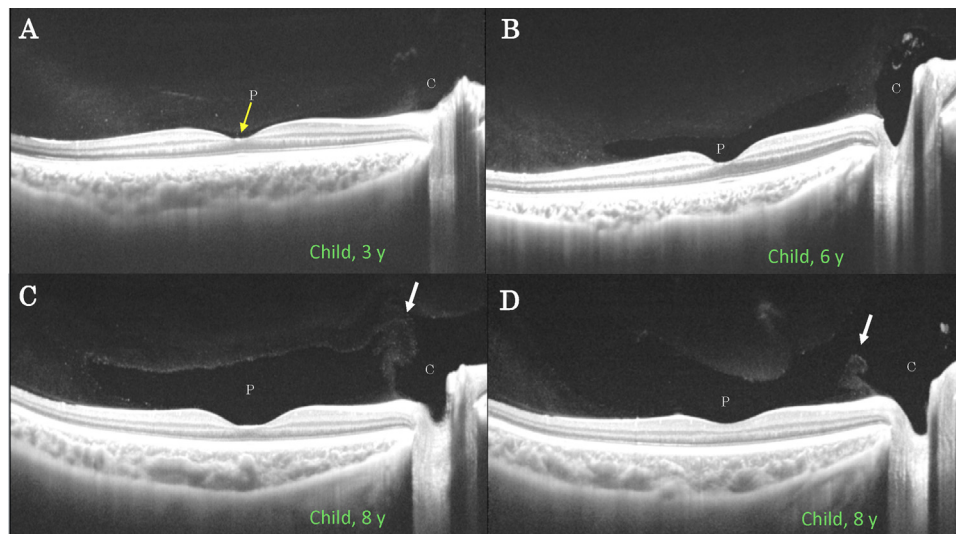


Figure 5. Evolution of the posterior precortical vitreous pocket (PPVP) during childhood. (A) In a 3-year-old child, the posterior precortical vitreous pocket (P) is the narrow space in front of the fovea. (B) In a 6-year-old child, the PPVP (P) is enlarged but smaller than in the adult. The PPVP and Cloquet's canal (denoted "C") appears to be independent. (C) In an 8-year-old, the PPVP is similar to the adult PPVP in size and shape. The connecting channel (arrow) is collapsed in the image. (D) The connecting channel (arrow) is opened. C = Cloquet's canal; P = posterior precortical vitreous pocket.

6. Fibrous structure of the vitreous

Eisner¹² described presence of vitreous veils and fibrous structure in the vitreous of adult humans. From the core of the vitreous to the cortical vitreous, these vitreous veils are named “tractus hyaloideus” (i.e., a wall of Cloquet’s canal), “tractus coronarius,” “tractus medianus,” and “tractus preretinalis”. Figure 6 shows a 40-year-old male who presented with metamorphopsia in his left eye. Spectral-domain optical coherence tomography revealed a perifoveal cyst and retinoschisis temporal to the macula; however, the vitreous was not clearly delineated. Swept source optical coherence tomography revealed a PPVP with a central dip in the gel and Cloquet’s canal. Retinoschisis was temporal to the macula with an inner columnar structure. There was a vitreous veil corresponding to the tractus preretinalis (Figure 6C). The vitreous cortex outside the tractus preretinalis was arranged in form of onion skin parallel to the fundus. The fibers in core side of tractus preretinalis were arranged perpendicularly.

7. The evolution of posterior vitreous detachment

Posterior vitreous detachment (PVD) is believed to be an acute event and has an increased incidence by the age of 60 years. Liquefaction of the vitreous gel precedes PVD. When liquefied humor escapes into the retrohyaloid space, the vitreous rapidly detaches from the retina, and the optic disc follows its collapse. However, Uchino et al¹³ reported that initial process of PVD starts in the perifoveal area and progresses to the focal PVD at the macula, which then develops to complete the PVD. By using the time domain OCT, Uchino could demonstrate the detached vitreous cortex; however, time domain OCT could not show any vitreous structure on the inner portion of the cortex. By using SD-OCT with

noise reduction, we investigated the manifestation of the PPVP in vitreomacular detachment in the eyes of 368 healthy volunteers (age range 12–89 years; mean age 57 years).¹⁴ The condition of the posterior wall of the PPVP was classified into five stages (Figure 7). Stage 0 was no PVD with PPVP (mean age 38.7 years). Stage 1 was paramacular PVD with PPVP (mean age 55.2 years). Stage 2 was perifoveal PVD with PPVP (mean age 62.0 years). Stage 3 was vitreofoveal separation with persistent attachment to the optic disc (mean age 65.8 years), which included stage 3a (i.e., vitreofoveal separation with an intact posterior wall of the PPVP) and stage 3b (i.e., vitreofoveal separation with a break in the posterior wall of the PPVP). Stage 4 was complete PVD (mean age 73.2 years). The pre-macular vitreous cortex is the posterior wall of the PPVP and consists of a collagen membrane. This specific nature of the pre-macular vitreous cortex and relatively strong attachment at the fovea constitutes the perifoveal PVD and trampoline-like macular PVD. The histogram shows a high incidence of partial PVD around the macula between the ages of 40 years and 60 years. This process precedes a complete PVD (Figure 8).

8. The role of the PPVP in vitreoretinal interface disorders

8.1. Idiopathic macular hole

Based on the PPVP, we proposed a mechanism of macular hole formation in 1996. This was well before the OCT was introduced.⁶ The pre-macular vitreous cortex corresponds to the posterior wall of the PPVP. If pre-macular vitreous cortex contracts tangentially, a trampoline-like PVD may develop. The vitreous cortex is strongly adherent to the fovea; therefore, a trampoline-like PVD may result in perifoveal PVD. In this situation, anterior traction persists at the fovea, which leads to foveal detachment, foveal cyst, and ultimately

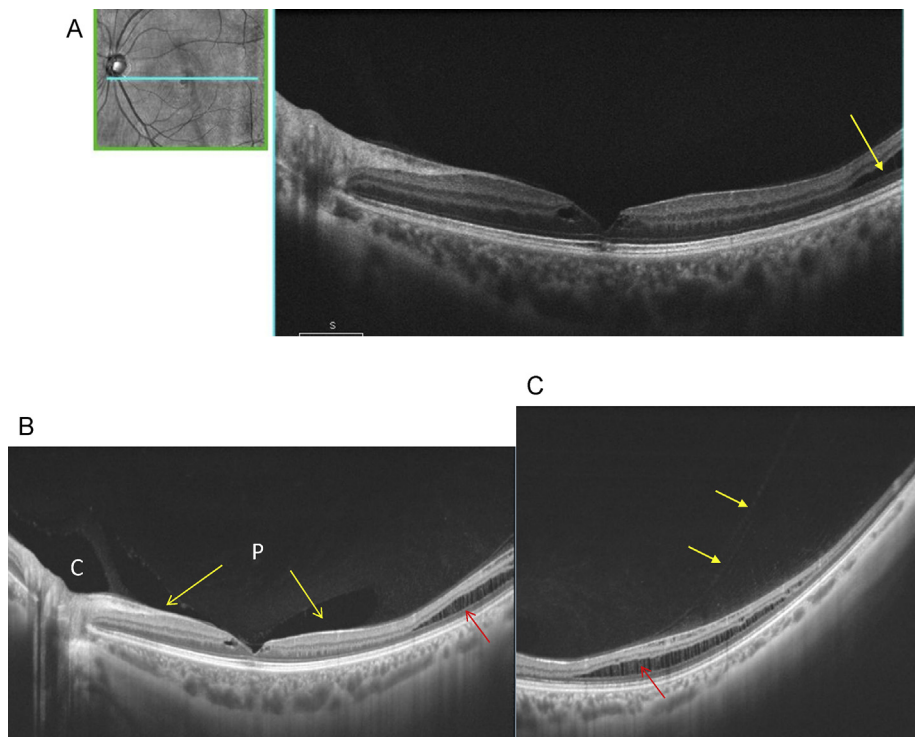


Figure 6. A 40-year-old male with a foveal cyst and midperipheral retinoschisis. (A) Horizontal section by spectral-domain OCT. Foveal cyst and retinoschisis (arrow) are visible. The vitreous structure is not visible. (B, C) Horizontal section by swept source OCT. (B) The posterior precortical vitreous pocket (P) with central depression is visible. Retinoschisis is clearly evident (red arrow). (C) The fibrous structure of the vitreous is visible. Tractus preretinalis (i.e., vitreous veil) is visible (yellow arrows). C = Cloquet’s canal; OCT = optical coherence tomography.

macular hole formation. The SS-OCT image confirmed the proposed mechanism of macular hole formation. Figure 9 shows a case of a Stage 1 macular hole in a 56-year-old man. At the initial visit, SS-OCT showed perifoveal PVD with foveal cyst. One month later, the foveal cyst had collapsed. At the 4th month, vitreoretinal attachment at the fovea was released. A trampoline-like PVD developed and resulted in the resolution of the macular cyst. The premacular vitreous cortex is the posterior wall of the PPVP (Figure 9C). Figure 10 shows a case of stage 3 macular hole in a 69-year-old male. The operculum is attached to the posterior wall of the PPVP.

8.2. Idiopathic epiretinal membrane

After examining the retinal surface of 59 postmortem eyes with PVD by scanning electron microscope, we found vitreous cortex remnants on the foveal surface in 26 (44%) eyes.¹⁵ This finding suggested that residual vitreous cortex may be a component of an idiopathic epiretinal membrane (ERM). After we reported the PPVP, we worked on the proposition that the posterior wall of the PPVP may be a part of the ERM. We found an oval defect of detached vitreous cortex in eyes with ERM and PVD.⁴ We assumed that the posterior wall of the PPVP remained on the macula during PVD. It then served as a collagen sheet for cellular proliferation (Figure 11). The posterior wall of the pocket exists as a collagen sheet before PVD; therefore, the ERM can develop on the posterior wall of a PPVP without PVD. Figure 12 shows a 52-year-old female who presented with ERM without undergoing PVD. When we performed SS-OCT, we found that the ERM was formed on the posterior wall of the PPVP.

8.3. Diabetic macular edema

Diabetic macular edema is also influenced by the PPVP (Figure 13). Perifoveal PVD can cause tractional cystoid macular

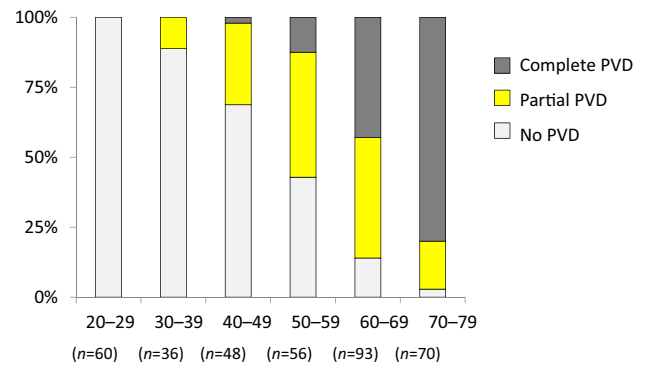


Figure 8. The incidence of partial and complete posterior vitreous detachment (PVD) in each decade of life.

edema (CME), which appears as solitary CME without exudative changes. When perifoveal PVD occurs, CME diminishes. The posterior wall of the PPVP may act as an ERM, which aggravates the diabetic macular edema.

9. Deep tissue penetration of SS-OCT

The light source of SD-OCT is a super-luminescent diode, which produces less tissue penetration than SS-OCT. The measurement beam of SD-OCT is blocked by retinal hemorrhage, exudates, and RPE; only the innermost layer of choroid is detected by SD-OCT. To overcome this limitation, Spaide introduced the technique of enhanced depth imaging, which allows visualization of the choroid. Swept source optical coherence tomography can depict the choroid and the tissue behind a dense hemorrhage without enhanced depth imaging.

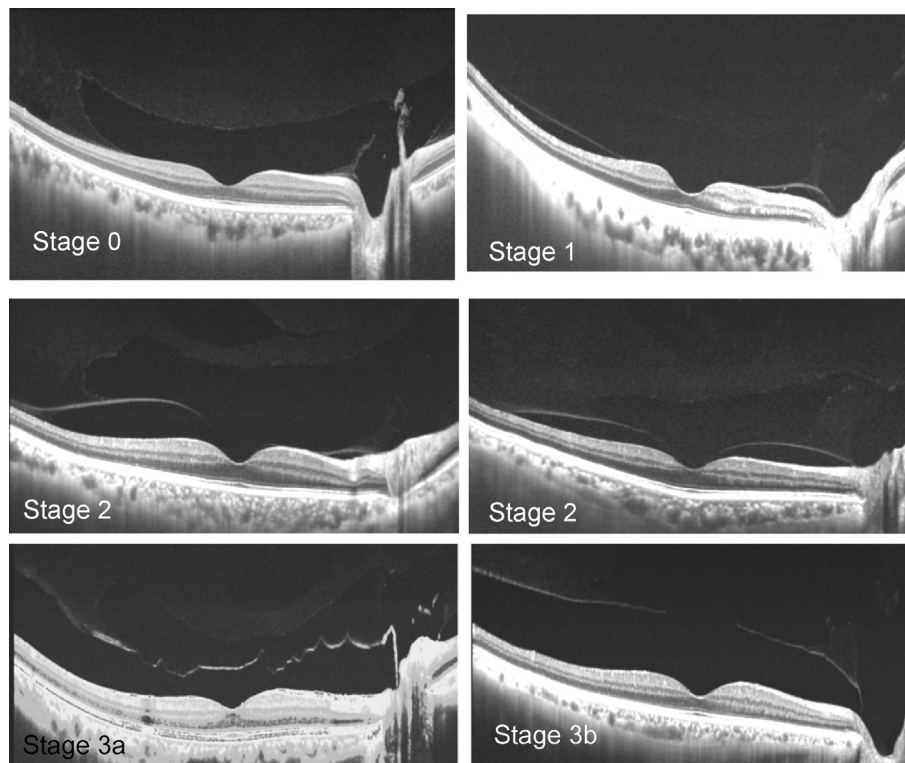


Figure 7. Evolution of physiological posterior vitreous detachment (PVD). Stage 0 is a posterior precortical vitreous pocket with no detached cortex. Stage 1 is focal PVD around the macula. Stage 2 is perifoveal PVD. Stage 3a is macular PVD with intact posterior precortical vitreous pocket (PPVP). Stage 3b is macular PVD with a break in the posterior wall of the PPVP.

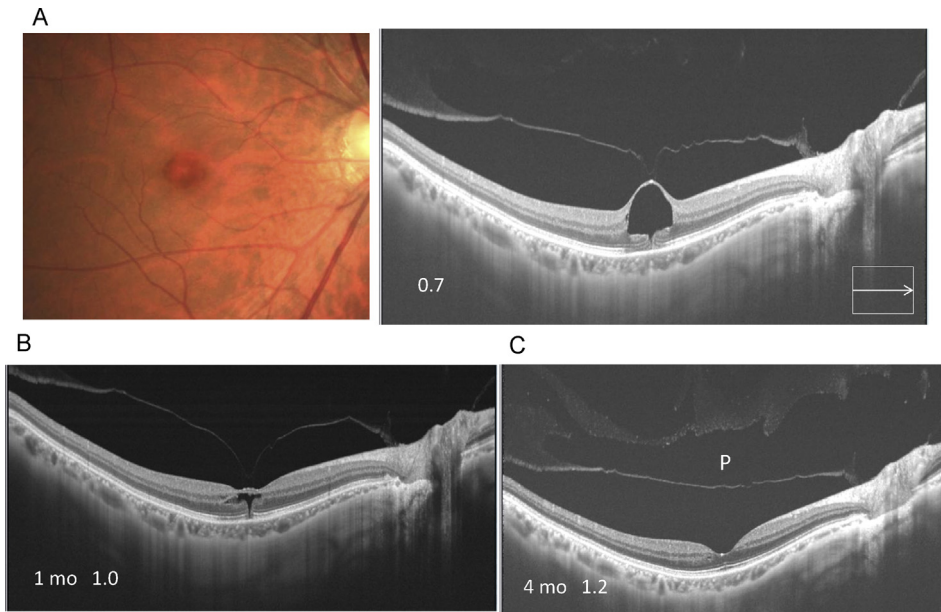


Figure 9. Stage 1 macular hole in a 56-year-old male. (A) At the initial visit, swept source optical coherence tomography shows perifoveal posterior vitreous detachment (PVD) and a foveal cyst. (B) One month later, the perifoveal PVD persists but the foveal cyst has collapsed. (C) Four months later, the vitreous cortex has detached from the macula and the foveal cyst is resolved. P = posterior precortical vitreous pocket. Values 0.7, 1.0 and 1.2 denotes decimal visual acuity.

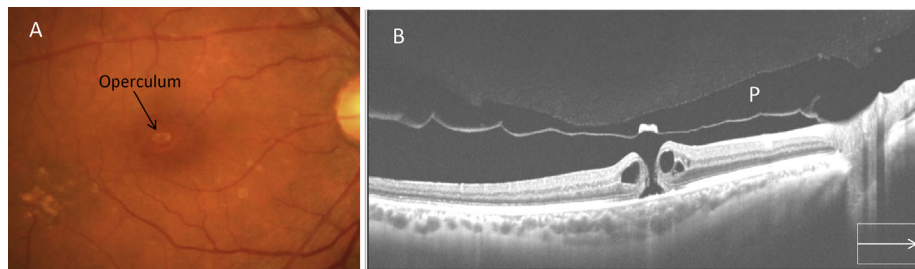


Figure 10. Stage 3 macular hole in a 69-year-old man. The operculum is attached on the posterior wall of the posterior precortical vitreous pocket (P). P = posterior precortical vitreous pocket.

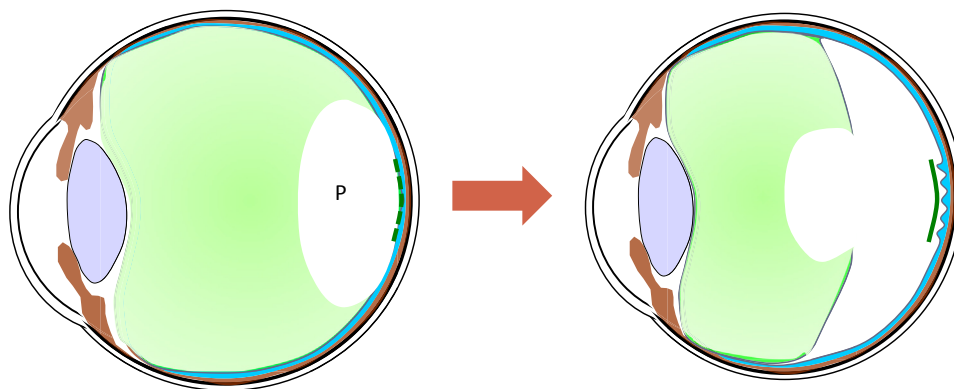


Figure 11. The possible mechanism of idiopathic epiretinal membrane (ERM). The posterior wall of the posterior precortical vitreous pocket (P) is a collagen sheet that serves as a structure of the ERM. When posterior vitreous detachment occurs, the posterior wall of the posterior precortical vitreous pocket may remain on the macula. Cellular proliferation on the collagen sheet may modify the nature of ERM. P = posterior precortical vitreous pocket.

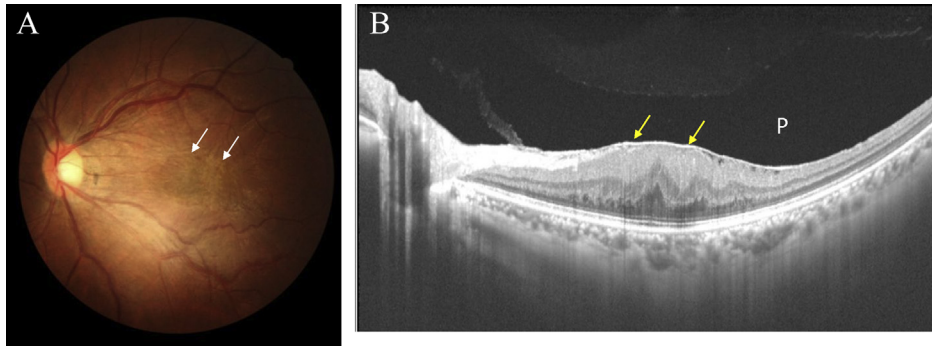


Figure 12. The epiretinal membrane (ERM) in a 52-year-old female. She has no posterior vitreous detachment. (A) Her left eye shows the ERM (arrows) in the macula. (B) Swept source optical coherence tomography shows that the thickened posterior wall (arrows) of the posterior precortical vitreous pocket (P) is itself the ERM. P = posterior precortical vitreous pocket.

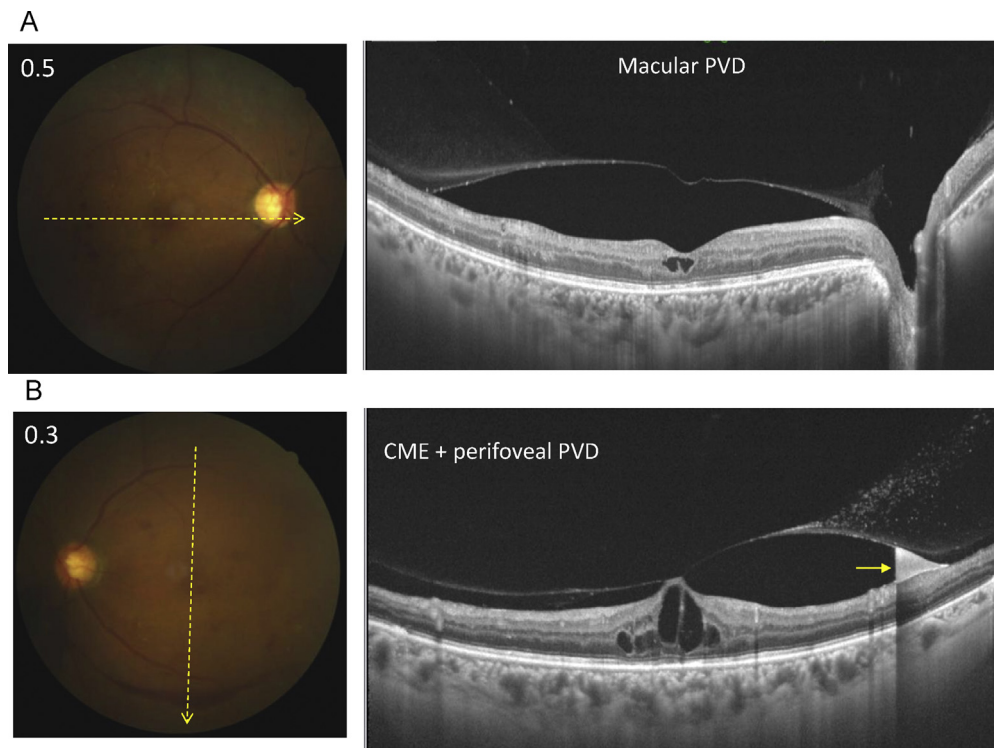


Figure 13. Diabetic retinopathy in a 45-year-old female. (A) In her right eye, posterior vitreous detachment has occurred in the macular area. Small cystoid macular edema (CME) is evident at the fovea. (B) In her left eye, crescent subhyaloid hemorrhage exists around the inferior vascular arcade. Swept source optical coherence tomography shows perifoveal posterior vitreous detachment with large CME and subhyaloid hemorrhage (yellow arrow). CME = cystoid macular edema; PVD = posterior vitreous detachment. Values 0.5 and 0.3 denotes decimal visual acuity.

9.1. Retinal arteriolar macroaneurysm

Figure 14 shows a case of a 79-year-old female with retinal macroaneurysm. Hemorrhages are located in subhyaloid, sub-internal limiting membrane (sub-ILM) and subretinal space. In SD-OCT, the inner feature of the hematoma is not visible. SS-OCT reveals subhyaloid hemorrhage, sub-ILM hemorrhage with clot and horizontal line, and subretinal hematoma (Figure 14C).

9.2. Polypoid choroidal vasculopathy

Exudative age-related macular degeneration is a complex lesion consisting of RPE detachment, sub-RPE choroidal neovascularization, polypoid lesions, and exudate or hemorrhages.

Figure 15 shows a case of polypoid choroidal vasculopathy (PCV) and subretinal hemorrhage in a 66-year-old man. Fluorescein angiography showed leakage from the subretinal mass. Indocyanine green angiography revealed a polypoid lesion and branching network of vessels. A diagnosis of PCV was determined. Despite the massive subretinal fibrin and hemorrhage, SS-OCT revealed serous RPE detachment, polypoid lesion, and the double layer sign in the RPE, which suggests sub-RPE choroidal neovascularization (Figure 15D).

9.3. Central serous chorioretinopathy

In the era of fluorescein angiography, the primary cause of central serous chorioretinopathy (CSC) may be the disruption of

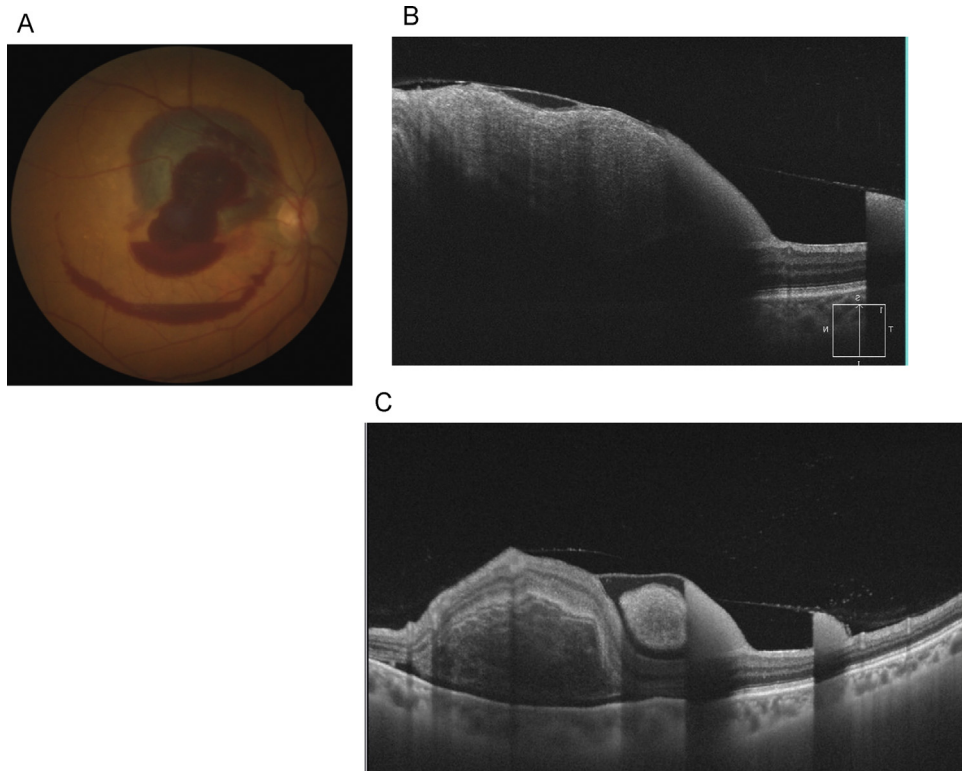


Figure 14. (A) Ruptured retinal macroaneurysm in a 79-year-old female. (B) In spectral-domain optical coherence tomography, the inner structure of the hematoma is not visible. (C) In swept source optical coherence tomography, the internal structure of the hematoma is visible.

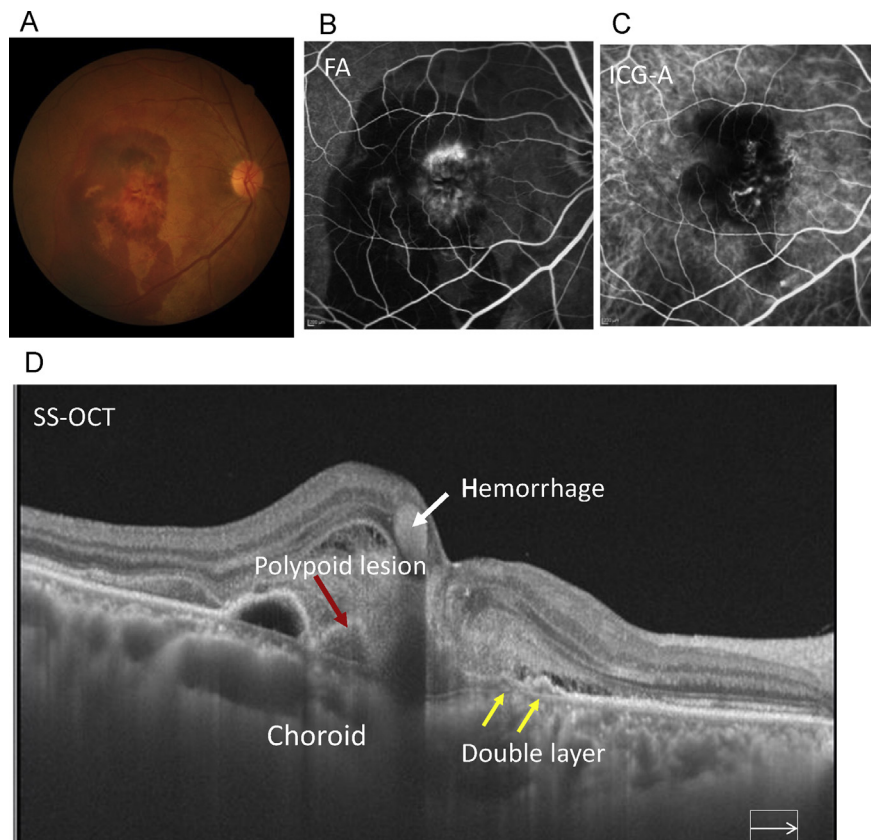


Figure 15. (A) Polypoid choroidal vasculopathy associated with subretinal hemorrhage in a 66-year-old man. (B) Fluorescein angiography image. (C) Indocyanine angiography image. (D) Horizontal section of swept source optical coherence tomography. FA = fluorescein angiography; ICG-A = indocyanine angiography; SS-OCT = swept source optical coherence tomography.

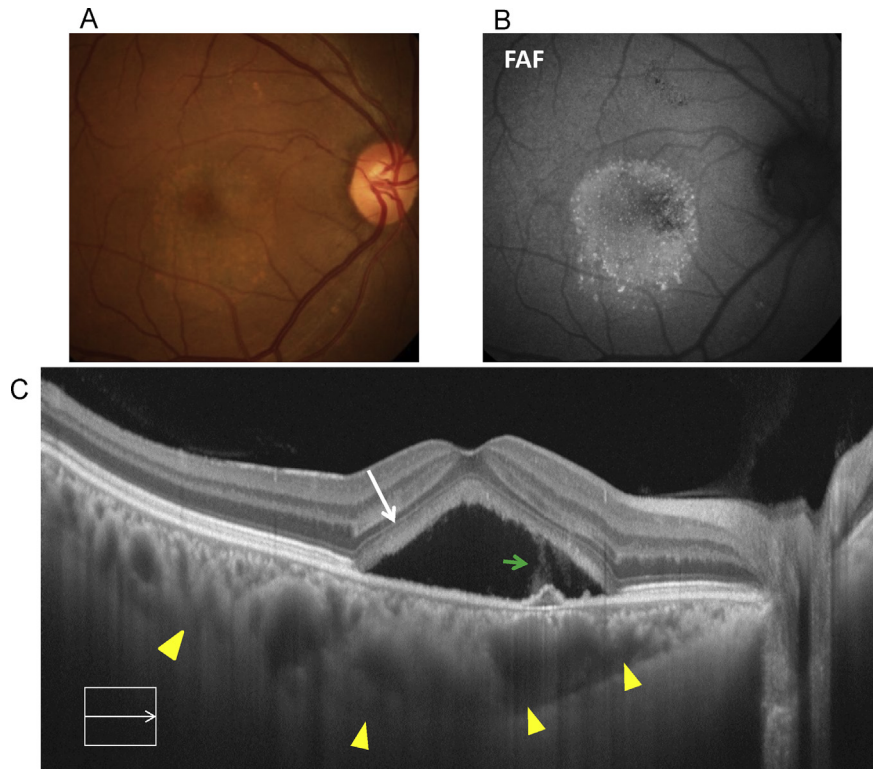


Figure 16. A 36-year-old male with acute central serous chorioretinopathy. (A) Serous retinal detachment with subretinal precipitates. (B) The precipitates emit autofluorescence. (C) Swept source optical coherence tomography shows marked swelling of the outer choroidal vessels (yellow arrowheads). In serous retinal detachment, photoreceptor outer segments are elongated (white arrow). Subretinal fibrin is visible (green arrow). FAF = fundus autofluorescence.

the outer blood retinal barrier of RPE from where choroidal fluid leaks and accumulates in the subretinal space. Indocyanine green angiography revealed dilated choroidal vessels with hyper-permeable dye in the choroid. Enhanced depth imaging in SD-OCT and SS-OCT revealed dilatation of outer choroidal vessels,

which may be vortex veins (Figure 16). The dilatation is pathognomonic for CSC. We now consider that congestion of the vortex veins may have a fundamental role in the pathogenesis of CSC. Subretinal fluid may be absorbed by focal laser photocoagulation, although choroidal swelling remains. However,

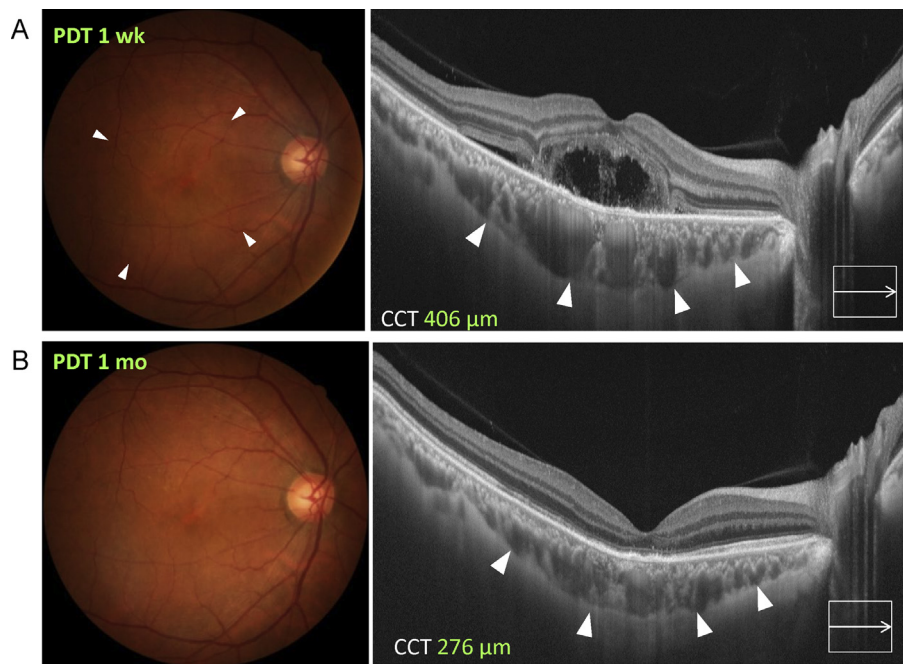


Figure 17. Acute central serous chorioretinopathy in a 56-year-old male. (A) One week after photodynamic therapy, choroidal swelling has decreased by approximately 10%. The outer choroidal vessels remain swollen. (B) One month later, the choroidal thickness has decreased to 276 μm and dilatation of outer choroidal vessels is diminished. CCT = central choroidal thickness; PDT = photodynamic therapy.

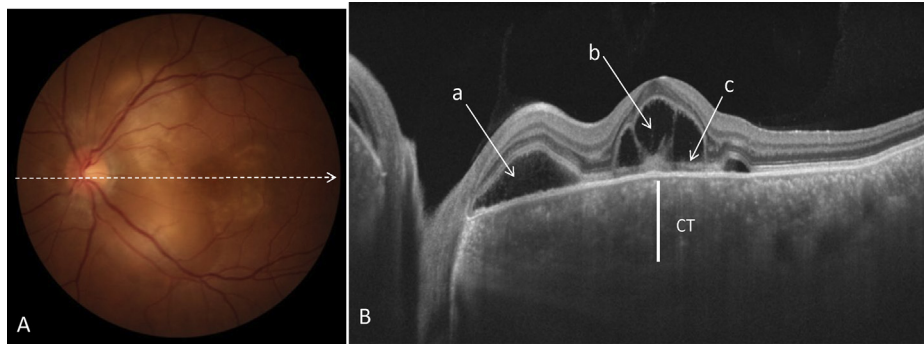


Figure 18. Harada disease in a 40-year-old woman. (A) The color fundus photograph shows serous retinal detachment in lobular pattern. Swept source optical coherence tomography reveals subretinal fluid (a), intraretinal fluid (b) and layer of the outer segment (c). The choroid is extensively swollen and the choriocleral border is not visible. CT = central choroidal thickness.

photodynamic therapy can diminish the swelling of the choroid¹⁶ (Figure 17).

9.4. Harada disease

Harada disease is also posterior uveitis with serous retinal detachment. In fluorescein angiography, the pooling of the dye frequently shows a lobular pattern, which differs from serous retinal detachment in CSC. Examination by SD-OCT and SS-OCT revealed that fluid can accumulate in the space between the detached outer segment of the photoreceptors and the retina; the space was surrounded by fibrin wall and the subretinal space (Figure 18).^{17,18} These spaces attributed the lobular pattern of dye pooling. Spectral-domain optical coherence with enhanced depth imaging or

SS-OCT revealed swelling of the choroid in the active stage of the choroiditis. Figure 19 shows a case of Harada disease in a 51-year-old man. At the initial visit, both eyes showed serous retinal detachments. The choroid was too swollen to detect the anterior border of the sclera, even by SS-OCT. The RPE overlying the swollen choroid is fluctuated. Three days after steroid pulse therapy (1.0 g of methylpredonolone for 3 d), choroidal swelling dramatically reduced to normal thickness in both eyes. However, 3 weeks after the steroid pulse therapy, exudative retinal detachment recurred in the left eye. His right eye had no recurrence but choroidal thickness remained remarkably increased, which suggested an impending relapse. We injected 30 mg of trimacinolone acetate into retrobulbar space in the right eye and left eye. We used SS-OCT to monitor the activity of Harada disease by observing the choroidal thickness on

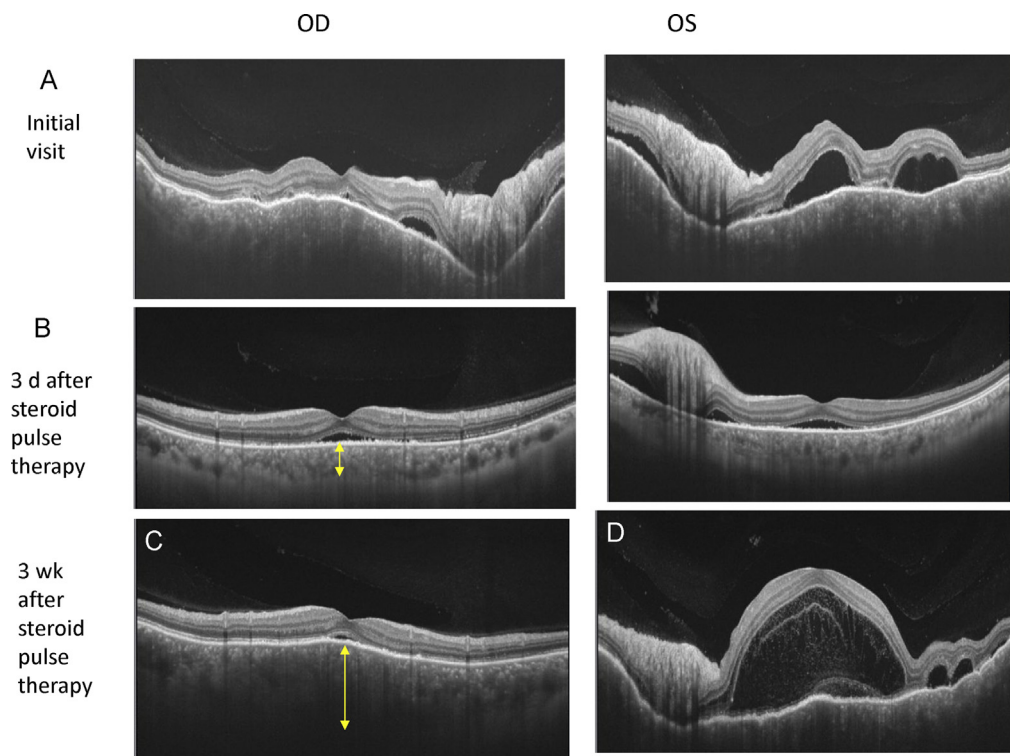


Figure 19. Harada disease in a 51-year-old female. (A) At the initial visit, both eyes have serous retinal detachment. The choroid is so swollen that the choriocleral border cannot be determined. (B) Three days after steroid pulse therapy, the subretinal fluid is remarkably absorbed. The choroid has reduced to normal thickness (yellow arrow). (C) Three weeks after steroid pulse therapy exudative retinal detachment recurred in the left eye. Fluid with fibrin has accumulated in the outer retinal space between the retina and detached outer segment. (D) The right eye shows no apparent recurrence; however, the choroid is remarkably thickened, which suggests an early relapse. OD = oculus dextrus; OS = oculus sinister.

SS-OCT. Thus, we can detect early signs of relapse and can treat it earlier, even before the visual symptoms develop.

References

1. Kishi S, Shimizu K. Posterior precortical vitreous pocket. *Arch Ophthalmol*. 1990;108:979–982.
2. Worst JG. Cisternal systems of the fully developed vitreous body in the young adult. *Trans Ophthalmol Soc U K*. 1977;97:550–554.
3. Worst J. Extracapsular surgery in lens implantation (Binkhorst lecture). Part IV. Some anatomical and pathophysiological implications. *J Am Intraocul Implant Soc*. 1978;4:7–14.
4. Kishi S, Shimizu K. Oval defect in detached posterior hyaloid membrane in idiopathic preretinal macular fibrosis. *Am J Ophthalmol*. 1994;118:451–456.
5. Kishi S, Shimizu K. Clinical manifestations of posterior precortical vitreous pocket in proliferative diabetic retinopathy. *Ophthalmology*. 1993;100:225–229.
6. Kishi S, Hagimura N, Shimizu K. The role of the premacular liquefied pocket and premacular vitreous cortex in idiopathic macular hole development. *Am J Ophthalmol*. 1996;122:622–628.
7. Sakamoto T, Miyazaki M, Hisatomi T, et al. Triamcinolone-assisted pars plana vitrectomy improves the surgical procedures and decreases the postoperative blood-ocular barrier breakdown. *Graefes Arch Clin Exp Ophthalmol*. 2002;240:423–429.
8. Fine HF, Spaide RF. Visualization of the posterior precortical vitreous pocket *in vivo* with triamcinolone. *Arch Ophthalmol*. 2006;124:1663.
9. Itakura H, Kishi S, Li D, Akiyama H. Observation of posterior precortical vitreous pocket using swept-source optical coherence tomography. *Invest Ophthalmol Vis Sci*. 2013;54:3102–3107.
10. Itakura H, Kishi S. Alterations of posterior precortical vitreous pockets with positional changes. *Retina*. 2013;33:1417–1420.
11. Li D, Kishi S, Itakura H, Ikeda F, Akiyama H. Posterior precortical vitreous pockets and connecting channels in children on swept-source optical coherence tomography. *Invest Ophthalmol Vis Sci*. 2014;55:2412–2416.
12. Eisner G. *Biomicroscopy of the Peripheral Fundus*. New York, NY: Springer-Verlag; 1979, 20,21,106,107.
13. Uchino E, Uemura A, Ohba N. Initial stages of posterior vitreous detachment in healthy eyes of older persons evaluated by optical coherence tomography. *Arch Ophthalmol*. 2001;119:1475–1479.
14. Itakura H, Kishi S. Evolution of vitreomacular detachment in healthy subjects. *JAMA Ophthalmol*. 2013;131:1348–1352.
15. Kishi S, Demaria C, Shimizu K. Vitreous cortex remnants at the fovea after spontaneous vitreous detachment. *Int Ophthalmol*. 1986;9:253–260.
16. Maruko I, Iida T, Sugano Y, Ojima A, Ogasawara M, Spaide RF. Subfoveal choroidal thickness after treatment of central serous chorioretinopathy. *Ophthalmology*. 2010;117:1792–1799.
17. Ishihara K, Hangai M, Kita M, Yoshimura N. Acute Vogt–Koyanagi–Harada disease in enhanced spectral-domain optical coherence tomography. *Ophthalmology*. 2009;116:1799–1807.
18. Yamaguchi Y, Otani T, Kishi S. Tomographic features of serous retinal detachment with multilobular dye pooling in acute Vogt–Koyanagi–Harada disease. *Am J Ophthalmol*. 2007;144:260–265.